Article **Journal of Mechanical Engineering**
December, 2023 Vol.7 No.20 28-35

Effect of design geometry on drag force in an experimental study on underwater drone

Efecto de la geometría del diseño en la fuerza de arrastre en un estudio experimental sobre un dron submarino

RODRIGUEZ-HIBERT, Cesar Francisco†*, RIVERA-LÓPEZ, Jesús Eduardo, GUTIÉRREZ PAREDES, Guadalupe Juliana and ARCINIEGA-MARTÍNEZ, José Luis

Instituto Politécnico Nacional, Escuela Superior de Ingeniería Mecánica y Eléctrica Unidad Azcapotzalco, México.

ID 1st Author: *Cesar Francisco, Rodriguez* / **ORC ID:** 0009-0003-1210-742X, **CVU CONAHCYT ID:** 1195667

ID 1st Co-author: *Jesús Eduardo, Rivera-López* / **ORC ID:** 0000-0003-3988-9305, **CVU CONAHCYT ID:** 161653

ID 2nd Co-author: *Guadalupe Juliana, Gutiérrez-Paredes* / **ORC ID:** 0000-0003-2918-7377, **CVU CONAHCYT ID:** 122745

ID 3rd Co-author: *José Luis, Arciniega-Martínez* / **ORC ID:** 0000-0003-4996-8146, **CVU CONAHCYT ID:** 161637

DOI: 10.35429/JME.2023.20.7.23.35 Received: September 30, 2023; Accepted: December 30, 2023

Abstract

Recently, underwater drones have known a growing interest, however, their design can still be improved to achieve higher autonomy and lower energy consumption. Therefore, this study focuses on studying the effect of design geometry on the drag force to improve the autonomy of drones by reducing their energy consumption. This study showed that the design geometry has a substantial influence on the drag coefficient reducing the drag effect by 13%. Experimental data demonstrated the dispersion of the drag coefficient as a function of the flow regime for each NACA profile used in the prototype. Also, it was found that the design geometry and the hydrodynamic efficiency of the drone are directly related, which means that with specific adjustments to the geometry a lower drag coefficient can be achieved. This study has shown that drag coefficient is a function of flow regime and that proper design can improve it. An optimized design would improve the range and efficiency of the drone by reducing power consumption due to lower drag force.

Drone, Drag coefficient, Towing tank

Resumen

Recientemente, los drones submarinos han conocido un interés creciente, sin embargo, su diseño aún puede mejorarse para conseguir una mayor autonomía y un menor consumo energético. Por ello, este estudio se centra en estudiar el efecto de la geometría del diseño sobre la fuerza de arrastre con el fin de mejorar la autonomía de los drones reduciendo su consumo energético. Este estudio demostró que la geometría de diseño tiene una influencia sustancial en el coeficiente de arrastre reduciendo el efecto de arrastre en un 13%. Los datos experimentales demostraron la dispersión del coeficiente de arrastre en función del régimen de flujo para cada perfil NACA utilizado en el prototipo. Asimismo, se ha comprobado que la geometría de diseño y la eficiencia hidrodinámica del dron están directamente relacionadas, lo que significa que con ajustes específicos en la geometría se puede conseguir un coeficiente de resistencia menor. Este estudio ha demostrado que el coeficiente de resistencia es función del régimen de flujo y que un diseño adecuado puede mejorarlo. Un diseño optimizado mejoraría la autonomía y la eficiencia del dron al reducir el consumo de energía debido a una menor fuerza de arrastre.

Dron, Coeficiente de arrastre, Tanque de remolque

Citation: RODRIGUEZ-HIBERT, Cesar Francisco, RIVERA-LÓPEZ, Jesús Eduardo, GUTIÉRREZ PAREDES, Guadalupe Juliana and ARCINIEGA-MARTÍNEZ, José Luis. Effect of design geometry on drag force in an experimental study on underwater drone. Journal of Mechanical Engineering. 2023. 7-20: 28-35

† Researcher contributing as first author.

1. Introduction

Underwater drones are novel devices within the field of aquatic vehicles, which play an important role in various application areas, such as marine exploration, aquatic monitoring, seabed mapping, ecosystem studies, etc. West et al., (2011). For this reason, the application of these devices requires various investigations concerning hydrodynamic efficiency, so a detailed analysis of the forces acting on drone hull geometries in various working conditions is needed since a poorly designed external geometry could cause high hydrodynamic drag Barlow et al., (2001).

The hydrodynamic drag is expressed in terms of the drag coefficient, $\boldsymbol{C_D}$, as shown by the results obtained Zihao et al., (2015), who presented an investigation on the measurement of $\boldsymbol{C_D}$, on 4 different geometrical bodies, by modifying the length-thickness ratio. The geometries were designed with wing shapes based on NACA (National Advisory Committee for Aeronautics) airfoils which were symmetric in the longitudinal plane and had chords ranging from $0.6\ to\ 1.2\ m$. In addition, two winglets were placed on each wing tip of the design.

The results obtained showed that the NACA66-023 profile of the 6 series reduces the hydrodynamic drag and stabilizes the boundary layer separation; and favors the increase of the internal volume to be able to install a greater amount of internal electronic components. It was also observed that the winglets reduce the $C_D$by 12.6% compared to the models that were tested without these profiles.

In this order, it was also studied by Javaid et al., (2017), the effect of the drag coefficient C_D of the geometry, for this purpose they designed an underwater drone and performed numerical and experimental tests in a towing tank, validating the numerical results by means of the experimental ones. The results show that the conical shape of the drone has a positive relationship with respect to drag reduction, for example, they observed that the drag force on an underwater device with wings with a rectangular shape is 15% higher compared to a device with conical shaped wings.

The above results are useful for designing drones efficiently. Two years later Praveen et al, (2019) elaborated a design of an underwater vehicle, with the objective of obtaining a geometry that produces a lower drag force, to decrease its energy consumption and improve autonomy and independence, designing a geometry with a partially cylindrical body and an elliptical shape at the rear, however, this geometry did not have the expected results, since, the results showed that for the tested speed range of 5, 10 and 15 m/s the drag force always increased by 152.4, 597.3 and 1101.1 N, respectively. Therefore, for this geometric design there was no drag reduction and therefore it should be optimized. In the same year another work was published by Javanmard and Mansoorzadeh, who presented results of the C_D of a prototype in a towing tank, obtaining a C_D= 0.23 at a speed of 2.5 m/s with a depth of 0.4 m, covering aspects such as; the length-diameter ratio, the shape of the body and the shape of the front part of the drone.

In addition, they studied the negative effects on the measurement of the drag force generated by the geometry of the connection of the trailer support with the model, having as a result that the percentage of error in the measurement of the force increases with the use of longer supports, and they also found that a support designed with the shape of a NACA 0012 profile generates 3 times less drag force compared to one designed in a circular shape at a depth of 0.6 m. The experimental $C_D$was compared with that obtained with *CFD* computational fluid dynamics, finding a maximum difference of 3.46%. Also, it was found that the difference between the numerical and experimental methods depend on the depth ratio and the velocity of the prototype in the towing tank. Similarly, Jagadeesh et al, (2009), conducted experiments with a prototype design with the characteristics of an autonomous underwater vehicle in a towing tank, comparing their results through *CFD* simulation, where they observed that at a Re of $1.05x10^5$ the experimental C_D is equal to 0. 0489 with a deviation of 0% with respect to the numerical simulation, otherwise, for a Re increase of $3.61x\ 10^5$,the $C_D$was 0.0389 with a deviation with respect to the numerical of 2.57 %, finding that for intermediate values of the interval $1.05x10^5 \leq Re \leq 3.61x\ 10^5$the $C_D$behaves with a deviation of less than 0.5% between the numerical and experimental tests.

ISSN-2531-2189

For the above, the research of Saeidinezhad et al., (2015) who performed aerodynamic tests of an asymmetric submersible vehicle in a wind tunnel, used as experimental similarity parameter the Reynolds number. Observing that the behavior of C_D increases for each increase of Re until reaching a flow regime of $5.9x10^6$, and for higher values of Re, $C_D$remains constant, C_D=1.18; finding that C_D ceases to be a function of Re after $5.9x10^6$, and therefore the drag achieves dimensionless independence from this flow regime, $C_D \neq f\ (Re)$. From the above, it was found that the tip of the device having an asymmetric shape generated a turbulent boundary layer, achieving stability in the $C_D$result at high flow regimes. This result was compared with the results obtained by Fidler et al; (1978) who analyzed in a wind tunnel bodies with different aerodynamic characteristics in a range of Re $4.0x10^6$to $8.5x10^6$, observing that the $C_D$presents a behavior similar to that reported by Saeidinezhad et al, (2015).

Therefore, this work aims to find the optimal geometry in the stern, which allows the reduction of drag due to the generation of vortices and thereby increase the independence, autonomy and useful work of an underwater drone to improve the operating time; according to Grant, S. (2019) this would allow installing novel technological devices such as sensors, sonars, high definition cameras promoting the development of underwater drones and their application.

2 Experimental Set-up

2.1 Concept design and additive manufacturing

For the purposes of this research work, a hydrodynamic prototype was developed using CAD software, in this first design stage an initial model of the physical configuration of the underwater device was obtained, culminating in the conceptual design of the drone. The result of this design process is shown in Figure 1, where the main dimensions of the hydrodynamic prototype are exhibited, which is constituted by an elliptical shaped bow to reduce drag; a main body of sufficient dimensions to contain the instrumentation, electronics, power source and energy source; a stern with a parabolic shape to reduce the generation of vortices.

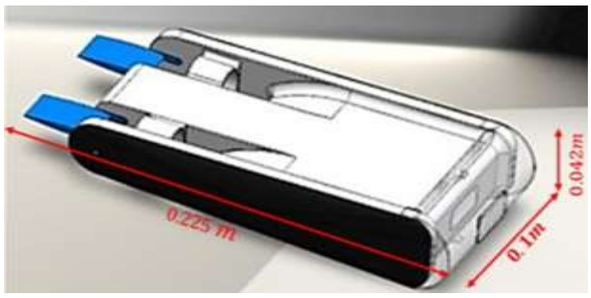

Figure 1 *CAD* model
Source: Own Elaborated

This design has as secondary elements symmetrical NACA profiles since they are widely used in the design of underwater vehicles (Gómez and Novella, 2021). According to Praveen et al. (2019), a good geometric design, is constituted with a parabolic bow and an elliptical stern, therefore, this work follows these recommendations. This work looks for an optimal geometrical design in the stern, therefore, it considers the study of two types of spoilers, which are based on NACA profiles of type 0010 and 0015. The selection of these two profiles is because they are symmetrical, stabilization of the boundary layer and decrease of adverse pressure gradients, according to the information provided by Garcia et al. (2014). The profiles will be exchanged in the main body, see Figure 2 and 3.

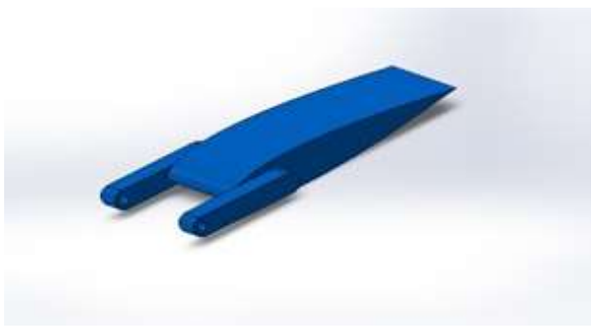

Figure 2 NACA profile 0010
Source: Own Elaborated

Figure 3 NACA profile 0015
Source: Own Elaborated

ISSN-2531-2189

Figure 4 shows the fabricated underwater device, which was made with additive manufacturing with the help of a 3D printer model X2, Artillery, in Basic AMAZON© PLA material, with a bending strength of 55.3 MPa, tensile strength of 57.8 MPa and a modulus of elasticity of 3.3 GPa. The fabrication was carried out in three phases, the first phase was the front cover, the second the main body and finally, the printing of the profiles.

Figure 4 Isometric view
Source: Own Elaborated

Figure 5 shows the spaces for the installation of the propellers and the slots designed for mounting the NACA profiles.

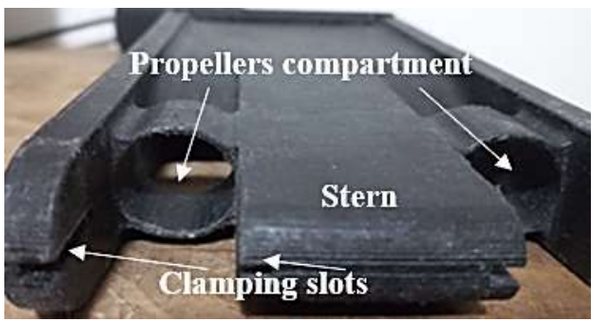

Figure 5 Stern of the experimental prototype
Source: Own Elaborated

For the execution of the experiments, the implementation of a designed and manufactured support was required to attach the prototype to the experimental bench. Following the recommendations of Javanmard and Mansoorzadeh (2019), a support with the geometry of the NACA 0012 profile was used. This approach aims at decreasing the drag force due to the support and consequently affecting the measurements on the main body of the Drone.

The support structure featured a 10 cm by 10 cm long rope, as shown in the physical arrangement depicted in Figure 6.

Figure 6 Model attached to the clamping support with NACA 0012 profile
Source: Own Elaborated

2.2 Experimental setup and test matrix.

The experimental tests were carried out on a towing tank operating in a speed range of 100 to 350 mm / s and the tank is 10 m long and has a cross section of 0.5 m, see Figure 6. The control of the towing carriage is by servomotor and the programming is by G-Code based algorithms, implemented from a computer. The trolley is equipped with a digital force sensor dynamometer with a maximum range of 32 N with an accuracy of 95%, the electrical output of the sensor is 35 Newtons at 5 volts.

The prototype is fixed to the NACA 0012 support, and in turn, this support is connected to the force sensor, the latter was positioned under the carriage thus ensuring a sturdy hold during the experimental tests, see Figure 7.

ISSN-2531-2189

To ensure a linear and parallel movement to the horizontal axis of the tank that does not generate lift forces on the NACA 0012 profile that affect the measurement of the drag force of the drone, the angle θ was adjusted, this was done with a digital level which aligned the profile with respect to the tank wall so that $\theta\ y\ \alpha \approx\ 0^0$, see Figure 8.

As part of the experimental methodology, tests were performed at seven different speeds, covering the operating range of the experimental bench from 100 to 350 mm/s (Martinez et al. 2016).

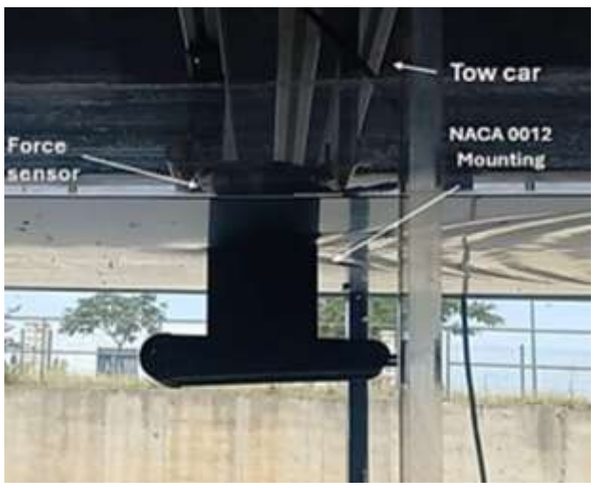

Figure 7 Prototype clamping
Source: Own Elaborated

Figure 8 Drone symmetry axes
Source: Own Elaborated

From the dimensional analysis the Reynolds number, Re, is the dimensionless parameter that will provide the dynamic similarity and therefore the full similarity of the experiment, equation 1.

$$Re = V.L/v \tag{1}$$

Where v is the kinematic viscosity of water equal to $8.83x10^{-4}\ \ kg/ms$, at test temperature 28.1 ºC, L is the characteristic length of the prototype and V is the test velocity.

The density of water at the test temperature is 996.03 kg/m^3.

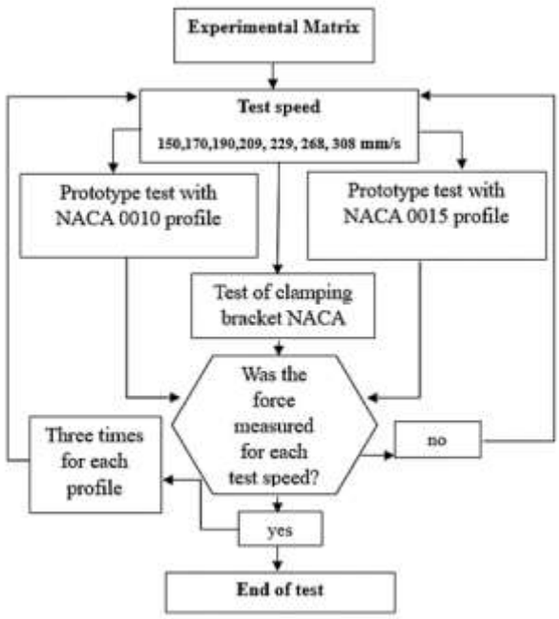

Figure 9 Experimental matrix
Source: Own Elaborated

In general, Figure 9 shows the test matrix that was developed for the measurement of the drag force of the prototype. Figure 10 shows schematically the experimental setup.

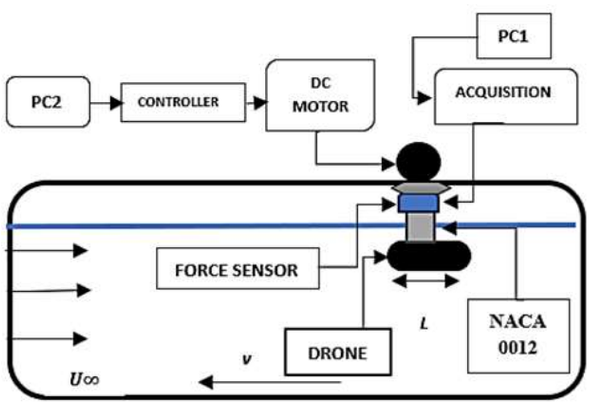

Figure 10 Scheme of the experimental setup
Source: Own Elaborated

ISSN-2531-2189

2.3 Experimental Runs

From the experimental runs performed, the results shown in Table 1 were obtained. With the test results, the net drag force of the prototype is calculated by means of equation 2.

$$F_{Dneta} = F_{Dexp}\text{-}F_{Ds} \quad (2)$$

Where the values of F_{Dnet} is the force acting on the prototype, F_{Dexp} is the measured force of the complete assembly and F_{Ds} is the force measured only for the support.

Medición No.	V (mm / s)	Naca 0010 F_D (N)	Naca 0015 F_D (N)	Naca 0012 F_D (N)
1	150	0.033	0.029	0.013
2	170	0.037	0.034	0.015
3	190	0.038	0.036	0.019
4	209	0.037	0.039	0.015
5	229	0.043	0.047	0.018
6	268	0.053	0.058	0.015
7	308	0.061	0.060	0.018

Table 1 Average results of the experimental measurement, F_D
Source: Own Elaborated

With the estimation of the drag force, the drag coefficient C_D can be calculated from the following equation 3, Cimbala (2016):

$$C_D = F_{Dneta}/0.5\rho U_\infty^2 A \quad (3)$$

Thus, ρ, U_∞ is the test velocity and A is the frontal area of the prototype which is equal to 42 mm^2.

3 Rsults

The results obtained are shown in graph 1.

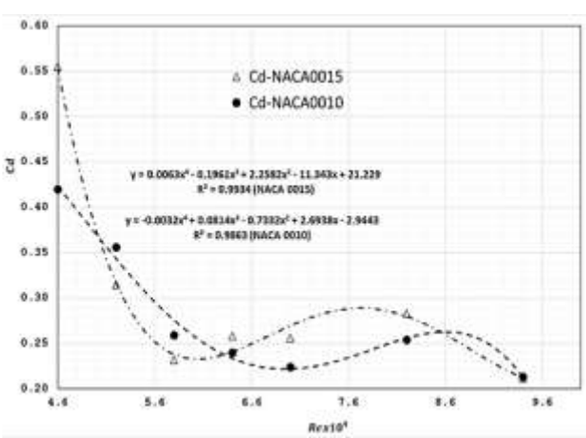

Graphic 1. C_D vs Re
Source: Own Elaborated

The graph shows the dispersion of the experimental data of the drag coefficient as a function of the flow regime of the prototype for each experimental arrangement of the NACA profiles.

As can be seen, the drag of the prototype with NACA 0015 is 23.6% higher than NACA 0010 at a Re of 4.6 X 10^4, but decreases 59% when Re increases up to , from this value of the flow regime the trend of the results shows that the asymptote begins to stabilize, since the slope of the curve almost disappears, therefore, if the flow regime continues to increase from this value of the Reynolds number the C_D will not have significant changes for the two experimental arrangements. The plot also shows the fit of the data for both experimental arrangements, see equations 4 and 5, these equations are the empirical models; the coefficient of quality of both equations is very close to one $R^2 \approx 1$, so, the quality of the data fit is assured.

$$C_D = 0.0063*Re^4\text{-}0.1961*Re^3 + 2.2582*Re^2\text{-}11.343*Re + 21.229 \quad (4)$$

$$C_D = 0.0032*Re^4\text{-}0.0814*Re^3 + 0.7332*Re^2\text{-}2.6938*Re + 2.9443 \quad (5)$$

Using the above equations, the experimental error is determined, see Table 2, which, the maximum error for the NACA 0010 arrangement is 6.07 % and for NACA 0015 is 52.8 %. It should be noted that the error for the NACA 0015 profile increases as the flow regime grows progressively and is maximum when the maximum test velocity is reached. In the case of the NACA 0010 profile the maximum error occurs when the Re is $5.8x10^4$ which is the value where the C_D begins to stabilize and as the results show, for each increase in velocity the error decreases with respect to the maximum error.

Re 10^4	NACA 0010 C_D %	NACA 0015 C_D %
4.6	0.72	2.27
5.2	3.64	7.41
5.8	6.07	15.14
6.4	2.58	11.91
7.0	0.67	25.54
8.2	1.53	32.32
9.4	2.04	52.79

Table 2 Error Experimental del C_D
Source: Own Elaborated

ISSN-2531-2189

It can be observed that the behavior of C_D has a coincidence with respect to the results of Jagadeesh et al. (2009) at intermediate Re numbers within the range of the experimental tests, behaving in a stable manner with both profiles.

Conclusions

From the results obtained from the test the following can be concluded:

1. In all the velocity range, the flow regime is laminar, therefore, the viscous forces predominated over the inertial ones, in the two experimental arrangements.

2. Therefore, in the whole test interval the prototype with the NACA 0015 arrangement has a higher drag compared to the other experimental arrangement.

3. On the contrary, the experimental arrangement with the NACA 0010 arrangement has a smaller drag.

4. In general, for the two experimental arrangements, there is an inflection point, since when reaching the flow regime $5.8x10^4$ the drag decreases and begins to stabilize and after this flow regime the C_D of the NACA 00010 arrangement is 13 % lower compared to the other experimental arrangement.

5. Finally, from the experimental error, it was observed that the arrangement with the NACA 0010 has the lowest experimental error compared to the other arrangement and therefore the best configuration is obtained when the prototype has the NACA 0010 profile at the stern.

Acknowledgments

We are very grateful to the University of Malaga, Spain for allowing us to use their facilities at the Vehicle Aerodynamics Laboratory (VAHL) and especially to the teaching staff for their facilities and help.

Funding

This work was carried out with financial resources provided by CONACHYT scholarships and Instituto Politecnico Nacional.

References

Barlow, JB, Gueterres, R. y Razenbach, R. (2001) Experimental parametric study of rectangular bodies with rounded edges on ground effect. J. *Eolico Idiana Aerodin*.

Cimbala, Ç, (2016) *Fluid Mechanics Fundamentals and Applications*. McGraw-Hill/Interamericana.

Fidler, J.E., Smith, C.A., 1978. Methods for predicting submersible hydrodynamic characteristics. NCSC/TM 238-78, July.

García-Ortiz, J. H., Domínguez-Vázquez, A., Serrano-Aguilera, J. J., Parras, L., & del Pino, C. (2019). A complementary numerical and experimental study of the influence of Reynolds number on theoretical models for wingtip vortices. *Computers & Fluids*, *180*, 176-189.

Gómez, J., y Novella, R. (2021). *Generador de perfiles NACA de 4 dígitos.* Polytechnic University of Valencia.

Grant, S. (2019). *Remote Explorer*. https://seagrant.mit.edu/auv-lab-vehicles/#early-vehicles / http://auvlab.mit.edu
Jagadeseh, P. y K. Murali (2009). Experimental investigation of hydrodynamic force coefficients over AUV hull form. *Ocean Engineering* 36(1), 113-118.

Javaid, M., Ovinis, M., Hashim, F. M., Maimun, A., Ahmed, Y. M., & Ullah, B. (2017). Efecto de la forma del ala sobre las características hidrodinámicas y la estabilidad dinámica de un planeador submarino. *International Journal of Naval Architecture and Ocean Engineering*, *9*(4), 382-389. https://doi.org/10.1016/j.ijnaoe.2016.09.01

Javanmard, E., & Mansoorzadeh, S. (2019). A computational fluid dynamics investigation on the drag coefficient measurement of an AUV in a towing tank. *Journal of Applied Fluid Mechanics*, *12*(3), 947-959. 10.29252/JAFM.12.03.29525

Martínez-Aranda, S., García-González, A. L., Parras, L., Velázquez-Navarro, J. F., & Del Pino, C. (2016). Comparison of the aerodynamic characteristics of the NACA0012 airfoil at low-to-moderate Reynolds numbers for any aspect ratio. *International Journal of Aerospace Sciences*, *4*(1), 1-8.

Praveen, V., Kishor, S., Sankaresh, K., Ashraf, E., & Thanga, K. (2019). Conceptual Design and Hydrodynamic Research on Unmanned Aquatic Vehicle. *International Journal of Innovative Technology and Exploring Engineering (IJITEE)*, 8, https://www.ijitee.org/wp-content/uploads/papers/v8i11S/K102709811S19.pdf

Saeidinezhad, A., Dehghan, A. A., & Manshadi, M. D. (2015). Experimental investigation of hydrodynamic characteristics of a submersible vehicle model with a non-axisymmetric nose in pitch maneuver. *Ocean engineering*, *100*, 26-34.

West, M., Collins, T., Bogle, J., Melim, A., & Novitzky, M. (2011). An Overview of Autonomous Underwater Vehicle Systems and Sensors at Georgia Tech. *Georgia Institute of Technology:* https://repository.gatech.edu/entities/publication/3ebd2ee2-0f02-4f7d-92e9-75000b356301

Zihao, W., Ye, L., Aobo, W., & Xiaobing, W. (2015). *Flying wing underwater glider: Design, analysis, and performance prediction.* IEEE

ISSN-2531-2189